Research Article

Tianjiao Zhang*, Yuelin Feng, Xinmin Ge, Wei Meng, Hongwei Han, Jingqiang Yu, Weizhong Zhang, Shuli Li, Xiaochen Li, and Ping Gao

Origin of carbonate cements in deep sandstone reservoirs and its significance for hydrocarbon indication: A case of Shahejie Formation in Dongying Sag

https://doi.org/10.1515/geo-2020-0283
received November 14, 2020; accepted July 20, 2021

Abstract: Carbonate cements are primary cement types formed in deep sandstone reservoirs of Dongying Sag. We have proposed three stages of carbonate cements with different origin and material sources: carbonate cements in early stage are rim-shaped high-Mg calcite, which is the product of quasi-contemporaneous period; and calcite filled with primary pores without obvious compaction and diagenetic transformation is mudstone compaction during the drainage process. Carbonate cements in middle stage are calcite and dolomite filled with feldspar secondary dissolved pores. The rich Ca^{2+}, Mg^{2+}, and CO_3^{2-} in overpressure fluid enter the reservoir and mix with Ca^{2+} in the original formation water. Carbonate cements in late stage are ferrocalcite and ankerite that filled the dissolution pores of early- and middle-stage carbonate cements. They were products of CO_3^{2-} formed by organic acid splitting decomposition in late diagenesis and CO_3^{2-} formed by dissolution of carbonate cements in early and middle stages, combined with Mg^{2+}, Ca^{2+}, Fe^{2+} plasma in pore fluid. Dissolution–reprecipitation of the lacustrine carbonate rocks is responsible for obvious positive drift in the $\delta^{13}C_{PDB}‰$ values of carbonate cements. Carbonate cements in middle stage and late stage, respectively, represent the early hydrocarbon charging of Dongying Formation and the end of Guantao Formation to the present.

Keywords: Dongying Sag, material sources, carbonate cements, hydrocarbon charging

1 Introduction

Carbonate cements are important type of cement in sandstone diagenesis demonstrating multistage precipitation, complex and diverse genesis, and wide distribution and can be generated in different geochemical environments [1–3]. Carbonate cements have become vital for understanding fluid–rock reaction systems. Material sources and precipitation mechanisms of such systems have been investigated based on microscopic mineral characteristics, fluid inclusion temperature measurement, isotopes, and other methods [4–8]. On the one hand, due to differences in material sources and precipitation mechanisms, different oxygen isotope values during the precipitation of diverse carbonate cements indicate the presence of different fluid–rock interaction systems and strengths [9]. During the primitive deposition period, mainly precipitated entities include quasi-syngenetic micrites, dolomite formed by oolites or cuttings, and early continuous calcite that filled the primary pores of sandstone particles. The formation temperature of such carbonate cements is generally low [5,10]; carbonate cements in the middle and late stages have relatively high inclusion temperatures, indicating that they precipitate at elevated temperatures during diagenesis [5,9]. However, material sources involved in redeposition-diagenesis mainly determine carbonate cement formation, such as Ca^{2+}, Mg^{2+}, Fe^{2+},

* **Corresponding author: Tianjiao Zhang,** Geophysical Research Institute, Sinopec Shengli Oilfield Company, Dongying, Shandong, 257022, China; Postdoctor Scientific Research Stations, Sinopec Shengli Oilfield Company, Dongying, Shandong, 257000, China, e-mail: tianjiaozhang0208@hotmail.com
Yuelin Feng, Wei Meng: Postdoctor Scientific Research Stations, Sinopec Shengli Oilfield Company, Dongying, Shandong, 257000, China; Research Institute of Petroleum Exploration and Development, Sinopec Shengli Oilfield Company, Dongying, Shandong, 257022, China
Xinmin Ge: School of Geosciences, China University of Petroleum (East China), Qingdao 266580, China
Hongwei Han, Jingqiang Yu, Weizhong Zhang, Shuli Li, Xiaochen Li, Ping Gao: Geophysical Research Institute, Sinopec Shengli Oilfield Company, Dongying, Shandong, 257022, China

CO_3^{2-}, and other materials [11,12]. On the other hand, hydrocarbon inclusions in the reservoir and associated brine inclusions reflect the history of oil and gas fluid formation [13]. In particular, fluid inclusions trapped in carbonate cements have the same temperature and salinity as those of oil and gas fluid filling and can simultaneously record the properties of filled oil and gas and diagenetic fluids. Therefore, combining these inclusions and carbonate cements can help to reveal hydrocarbon charging in sedimentary basins [14,15], which has important theoretical and practical significance for oil and gas exploration.

In this work, we investigated the vertical distribution, stages, material composition, and carbonate cement sources in different layers of Dongying Sag in Bohai Bay Basin. The material sources and genesis of carbonate cements as well as their relationship with fluid inclusions are discussed based on carbonate cement petrology, mineralogy, carbon and oxygen isotopes, and homogenization temperature of inclusions using electron probe trace element analysis. The combined method is used to understand the relationship between the formation of carbonate cements in sandstone and fluid activities under deep burial conditions.

2 Geological settings

Dongying Sag is located in the southeast of Bohai Bay Basin, bordered by Chenjiazhuang uplift to the north, Binxian and Qingcheng uplifts to the west, Luxi and Guangrao uplifts to the south, and Qingtuozi uplift to the east (Figure 1a and b) with an area of 5,700 km^2 and is a half graben-like fault basin, including Lijin Sub-sag, Dongying Sub-sag, Boxing Sub-sag, Minfeng Sub-sag, and the central fault belt (Figure 1c and d).

The Cenozoic is the main stage of the formation and evolution of Dongying Sag with intense structural activities and a set of thick continental clastic deposits [16–19], including Kongdian (Ek), Shahejie (Es), Dongying (Ed), Guantao (Ng), Minghuazhen (Nm), and Plain (Qp) Formations. Shahejie Formation can be further subdivided into four members from the top to the bottom: Es1, Es2, Es3, and Es4, respectively. In this work, we focused on Es4 and Es3.

The thickness of Es4 can reach 1,500–1,600 m, generally showing a complete coarse-fine-coarse cycle. The lower member of Es4 is composed of purple-red mudstone with brown siltstone, sandy mudstone, and thin carbonate rocks. The upper member of Es4 is composed of dark gray mudstone and shale. The thickness of Es3 is generally 700–1,000 m with the thickest part exceeding 1,200 m. It is mainly composed of gray and dark gray mudstone with sandstone, shale, and carbonaceous mudstone. Es2 is mainly composed of gray mudstone, sandstone, and gravel-bearing sandstone, while Es1 gray and dark gray mudstone, oil shale, and carbonate rock (Figure 2).

3 Methods

The samples were mainly collected from Shahejie Formation in Dongying Sag. Thin-section casting, quantitative statistics, cathodoluminescence, scanning electron microscopy, homogenization temperature testing, carbon and oxygen stable isotope testing, and electron probe analysis were used. All analyses and testing work were completed in the Petroleum Geology Testing Center of the Exploration and Development Research Institute of Sinopec Shengli Oilfield Co Ltd.

3.1 Type and occurrence analysis of carbonate cements

Two hundred and fifteen core samples from 60 wells in Dongying Sag were selected. Blue epoxy resin was used to polish cast sections stained with alizarin red, and the cast sections were identified by Leize polarized light microscope. At the same time, 63 typical samples were selected, and the thermal cathodoluminescence analysis and dyeing analysis of the cast thin sections were performed by cathodoluminescence (CL8200 MK5) to identify the types of carbonate cements in the core samples. The occurrence of carbonate cements and the contact accountability relationship were completed by a field emission environmental scanning electron microscope (Quanta450FEG/-J).

3.2 Electron probe analysis of carbonate cements

Sixty samples from 20 wells were selected. Electron probe microanalysis (JEOLJXA-8230) was performed to quantitatively test the chemical compositions of carbonate

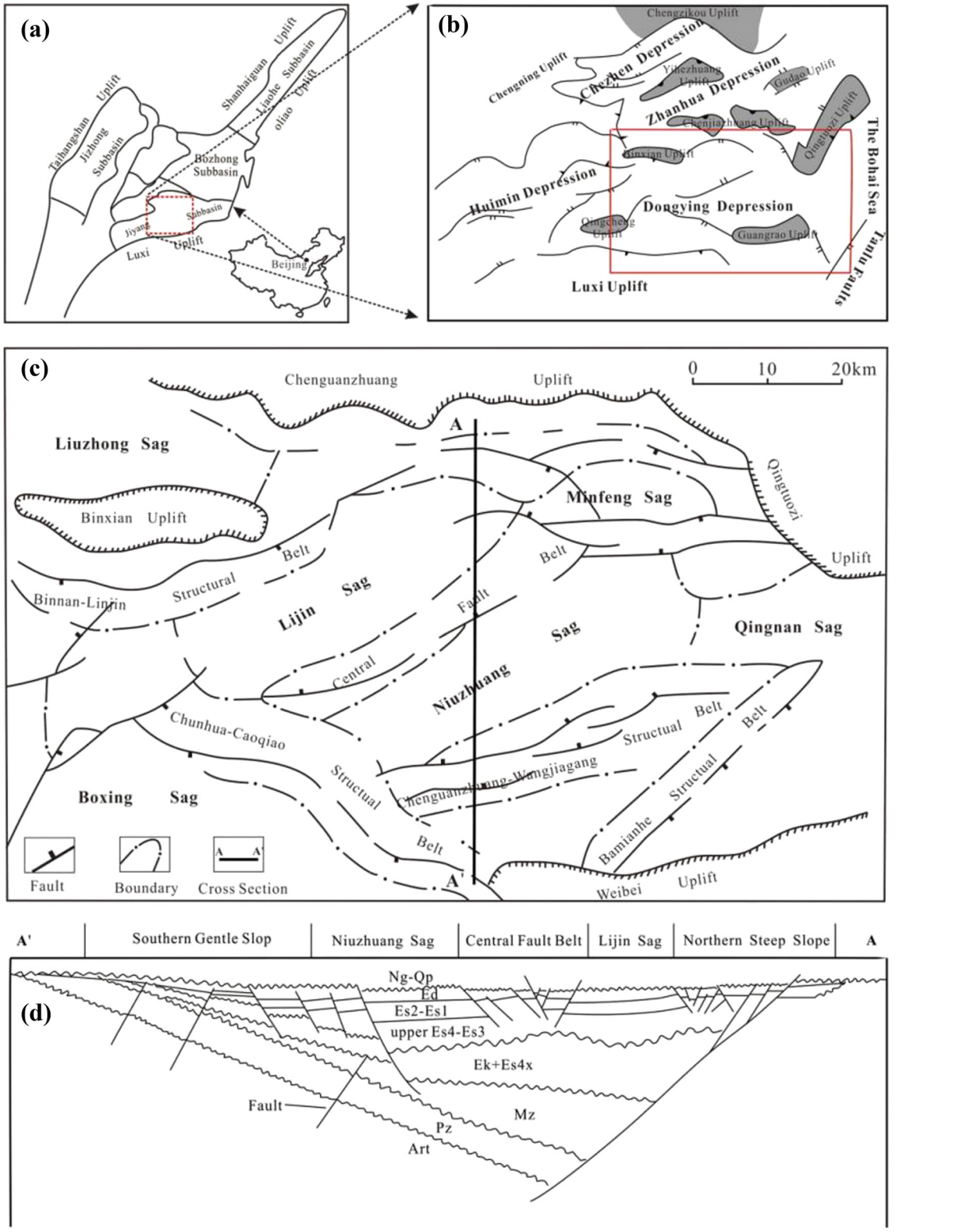

Figure 1: (a) Structural map of Bohai Bay Basin. (b) Tectonic setting of the Jiyang Depression. (c) Tectonic setting of Dongying Sag and the locations of sections AA′. (d) Cross section of sections AA′ showing the tectonostructural zones within Dongying Sag.

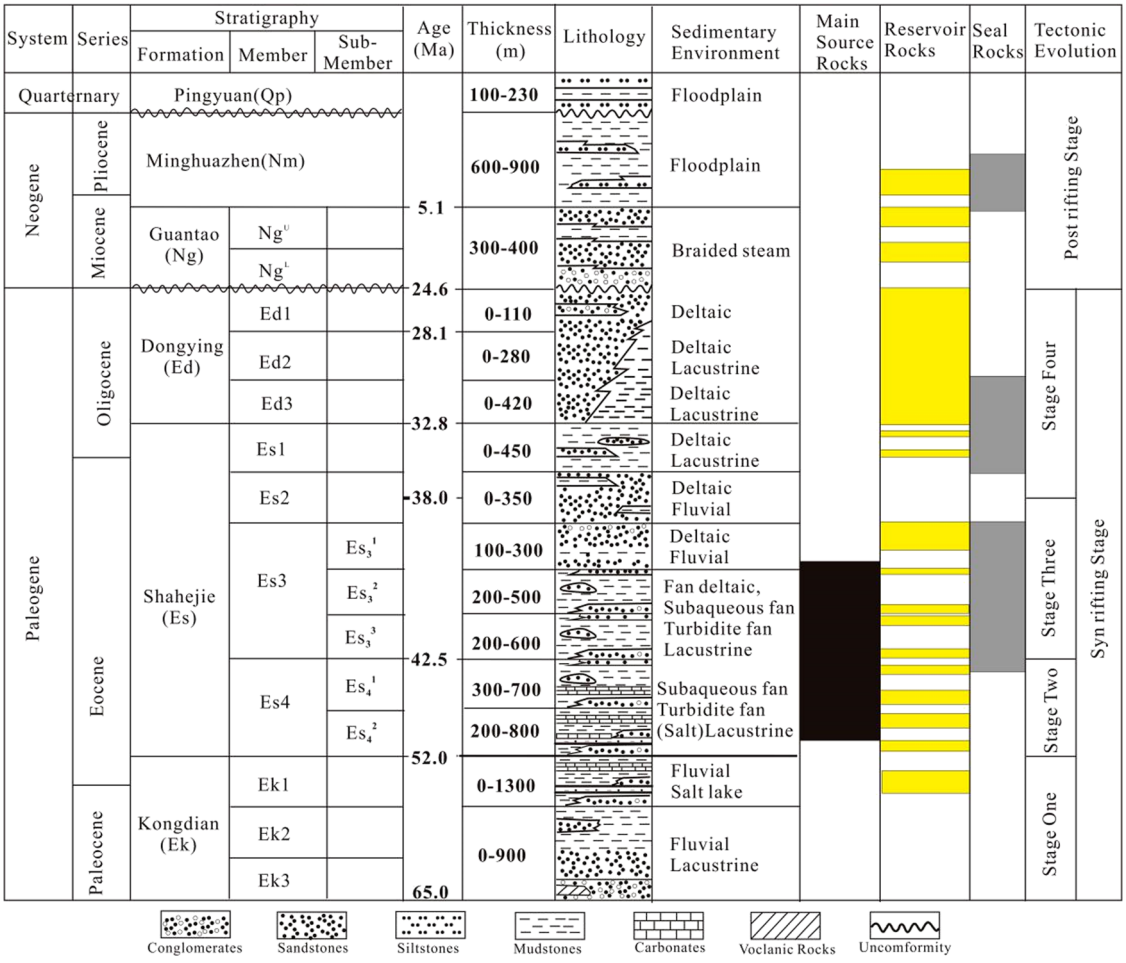

Figure 2: Generalized Cenozoic-Quaternary stratigraphy of Dongying Sag.

cements and conduct an elemental surface analysis. The main elements tested include four elements: Ca, Mg, Fe, and Mn. The analysis error was less than 3%.

3.3 Homogenization temperature testing of inclusions

Hundred core samples from 30 wells were selected to prepare double-polished slices with a thickness of 100 m to test the homogenization temperature of fluid inclusions and clarify the formation temperature and time of carbonate cements. The petrographic characteristics of fluid inclusions were observed using a polarized reflective fluorescent microscope (ZEISS DMR XP). The homogenization temperature measurement was performed on the cold and hot table (LinKam-THMS600). The refrigerant used in the test was liquid nitrogen, and standard sample calibration was performed at –196 to 600°C with an error of 0.1°C. The temperature control rate was 1–10°C/min, the room temperature was 25°C, and the humidity was 65%.

3.4 Carbon and oxygen stable isotope testing of carbonate cements

The corresponding carbonate cements from sandstone samples were dried in the air, grounded to 200 mesh, and reacted with 100% phosphoric acid, and the released CO_2 was collected. A gas isotope mass spectrometer (MAT253) was used to test the stable isotopes of carbon and oxygen.

4 Results

4.1 Types and occurrence of carbonate cements

The morphological and geochemical characteristics of carbonate cements in the sandstone of Shahejie Formation in Dongying Sag were studied by thin-section casting, cathodoluminescence, backscattering, electron probe analysis, and isotope analysis. Optical microscopy and cathodoluminescence results indicated carbonate cementation in the sandstone of the deep Shahejie Formation in Dongying Sag, and mainly, early-stage calcite, middle-stage calcite and dolomite, and late-stage ferrocalcite and ankerite were found.

The carbonate cements in the early stage are mainly calcite, which can be divided into two types based on their production: the first type is mainly micritic high magnesium calcite, which usually has a good degree of automorphism, and is mostly in the form of micritic equal thickness rim, which is semi-basal-basal cementation and occurs on the surface of a small amount of clastic rock particles (Figure 3a). The second type is mainly microcrystalline calcite, mostly developed between clastic grains (Figure 3b), and the cathodoluminescence is orange (Figure 3c). Microscopic observation showed that the clastic particles were mainly distributed in the carbonate cements of this period in the form of point contact or floating, and no feldspar particles were dissolved or metasomatism clastic particles appeared. Meanwhile, the intergranular pores were relatively developed, indicating that the clastic particles had not been modified by compaction, so the formation time was earlier. The carbonate cements in the middle stage are mainly microcrystalline fine-grained calcite and dolomite. Different from carbonate cements in the early stage, carbonate cements in the middle stage are mostly dispersed and filled with pores, occupying the dissolution space of feldspar, and the secondary increased edge phenomenon of metasomatized feldspar grains and quartz can be seen (Figure 3d–f); the cathode luminescence is orange-yellow and dark red (Figure 3i). The clastic grains are mostly in point-line contact to lineal contact, which indicates that the sandstone has been strongly compacted and the cements precipitated after the dissolution of feldspar, and the precipitation time is later than that of carbonate cements in the early stage, indicating that this period is later than the formation period of carbonate cements in the early stage. The carbonate cements in the late stage are mainly fine-grained ferro-calcite and ankerite, which are porous cementation. The clastic particles are closely arranged and mostly in line contact, indicating that the sandstone has been strongly compacted and transformed; it mainly occupies the dissolution space of feldspar, carbonate cement in the early and middle stage, and some metasomatize feldspar particles and quartz enlarge edge (Figure 3e, g, and h); under cathodoluminescence, ferrocalcite is dark orange-yellow, while ankerite does not emit light (Figure 3i), indicating that it was formed later.

4.2 Chemical composition of carbonate cements

Electron probe microanalysis and energy spectrum analysis were used to observe and identify different types of carbonate cements in the deep sandstone reservoirs of Dongying Sag and analyze their major element components. The results showed that calcite in the early stage is distributed in ring-shaped aggregates with a chlorite layer on the surface and demonstrated symbiosis with a small amount of authigenic early-stage pyrite particles (Figure 4a). The composition of carbonate cements in this stage is characterized by high-Ca, medium-Mg, and low-Fe (Figures 4b and 5): $CaCO_3$ content was 65.35–75.15% with an average of 71.95%, $MgCO_3$ content was 21.04–33.87% with an average of 27.11%, $FeCO_3$ content was 0.46–1.47% with an average of 0.93%, and $MnCO_3$ content was 0.00% (Table 1), indicating that this type of carbonate cement is micritic high-Mg calcite.

The second type of carbonate cements in the early stage fills the primary pores without obvious compaction and diagenetic transformation (Figure 4d). The composition of this carbonate cement is characterized by high Ca, low Mg, and low Fe (Figures 4c and 5). The content of $CaCO_3$ was 86.75–96.11% with an average of 90.38%; the content of $MgCO_3$ was 3.10–12.77% with an average of 8.85%; the content of $FeCO_3$ was 0.48–0.98% with an average of 0.77%; the content of $MnCO_3$ was 0.1–0.12% with an average of 0.05% (Table 1), indicating that this type of carbonate cement is calcite.

The carbonate cements in the middle stage are mostly filled with feldspar dissolved and compacted in residual pores (Figure 4d and g); carbonate cements in this stage can be divided into two types. The first type is characterized by high Ca, medium-low Mg, and low Fe (Figures 4e and h and 5). The content of $CaCO_3$ was 95.71–99.44% with an average of 97.89%, $MgCO_3$ content was 0.00–2.12% with an average of 0.74%, $FeCO_3$ content was 0.17–2.17% with an average of 1.17%, and $MnCO_3$ content was 0–0.22% with an average of 0.07%, indicating that

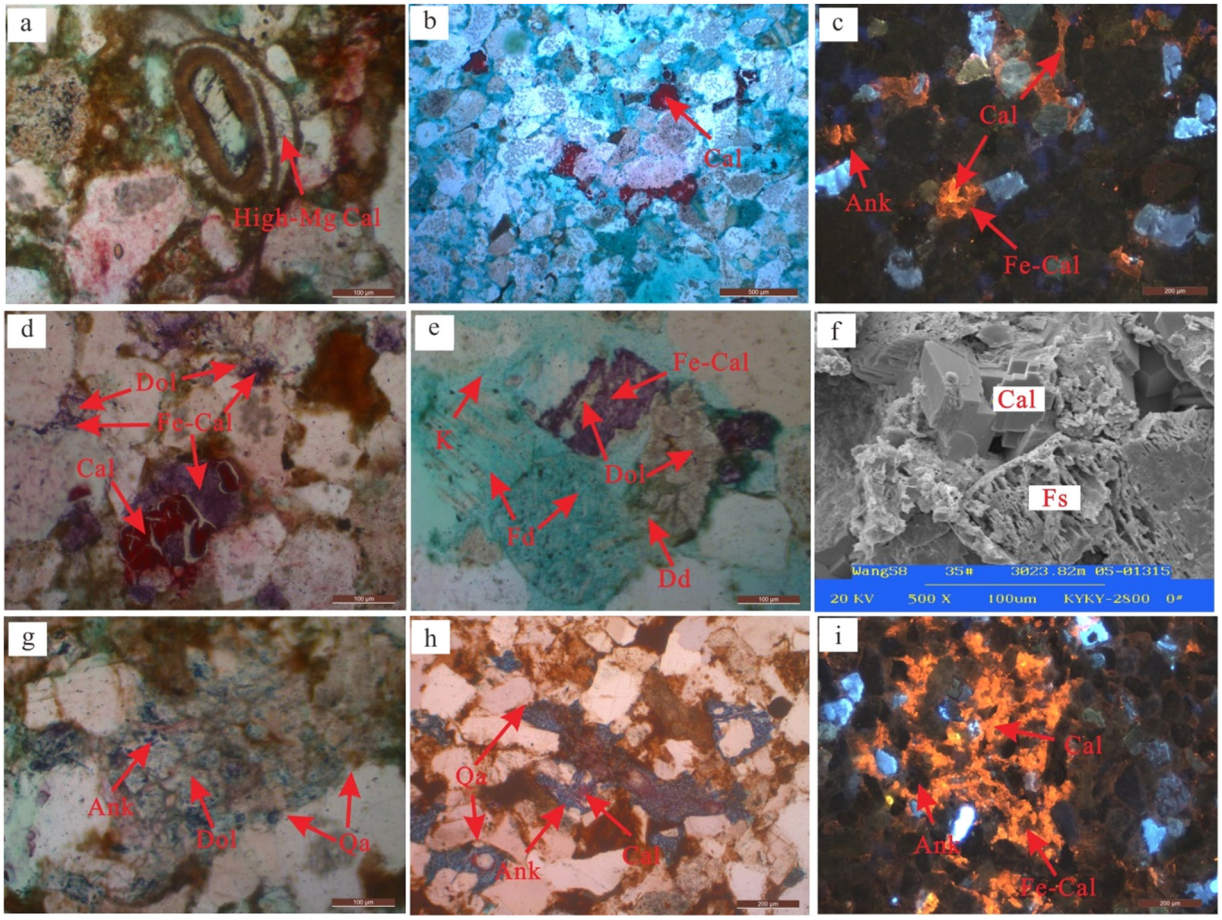

Figure 3: Diagenesis micrograph of carbonate cements in Dongying Sag. (a) N105, 3251.66 m, micritic high-Mg calcite in early stage; (b) X154, 2934.50 m, calcite in early stage filled primary pores; (c) X154, 2934.50 m, calcite in early stage, the cathodoluminescence was bright orange-yellow; (d) G110, 2671.93 m, ferro-calcite in late stage filled the dissolution pores of calcite and dolomite in middle stage; (e) W541, 3132.98 m, dolomite in middle stage filled dissolution pores of debris, and the later dissolution was filled by ferro-calcite in late stage; (f) W58, 3023.82 m, calcite in middle stage filled feldspar dissolution pores; (g) N21, 3431.50 m, dolomite in middle stage filled the dissolution pores of feldspar particles and metasomatized part of quartz secondary enlarged edge, later was metasomatized by ankerite in late stage; (h) N24, 3174.85 m, ankerite in late stage filled the dissolution pores of calcite in middle stage and metasomatizes quartz secondary enlarged edge; and (i) W631, 3243.80 m, the cathodoluminescence of ferro-calcite is dark orange red, while ankerite does not emit light.

this type of carbonate cement is calcite. The second type is characterized by medium-low Ca, high Mg, and low Fe in which $CaCO_3$ content was 31.24–51.80% with an average of 44.91%, $MgCO_3$ content was 46.04–68.30% with an average of 54.51%, $FeCO_3$ content was 0.23–1.03% with an average of 0.57%, and $MnCO_3$ content was 0.00% (Table 1), indicating that the type of carbonate cement is dolomite.

The carbonate cements in the late stage are mainly filled with the dissolution pores of early- and middle-stage calcite and dolomite (Figure 4d and g), and the clay-mixed layer minerals of illite and montmorillonite and high automorphic silk illite are developed on their surface. Two types of carbonate cements were identified in this stage. The first type is characterized by high Ca, medium-low Mg, and high Fe (Figure 4f). The content of $CaCO_3$ was 84.59–90.55% with an average of 87.01%; the content of $MgCO_3$ was 0.00–1.79% with an average of 1.10%; the content of $FeCO_3$ was 8.40–15.41% with an average of 11.89%; the content of $MnCO_3$ was 0.00%, indicating that it is iron calcite. The second type is characterized by medium-low Ca, high Mg, and high Fe (Figures 4i and 5) in which $CaCO_3$ content was 50.68–60.25% with an average of 56.77%; $MgCO_3$ content was 23.13–36.92% with an average of 28.45%; $FeCO_3$ content was 11.27–15.73% with an average of 13.78%; $MnCO_3$ content was 0–1% with an average of 0.57% (Table 1), indicating that it is ankerite.

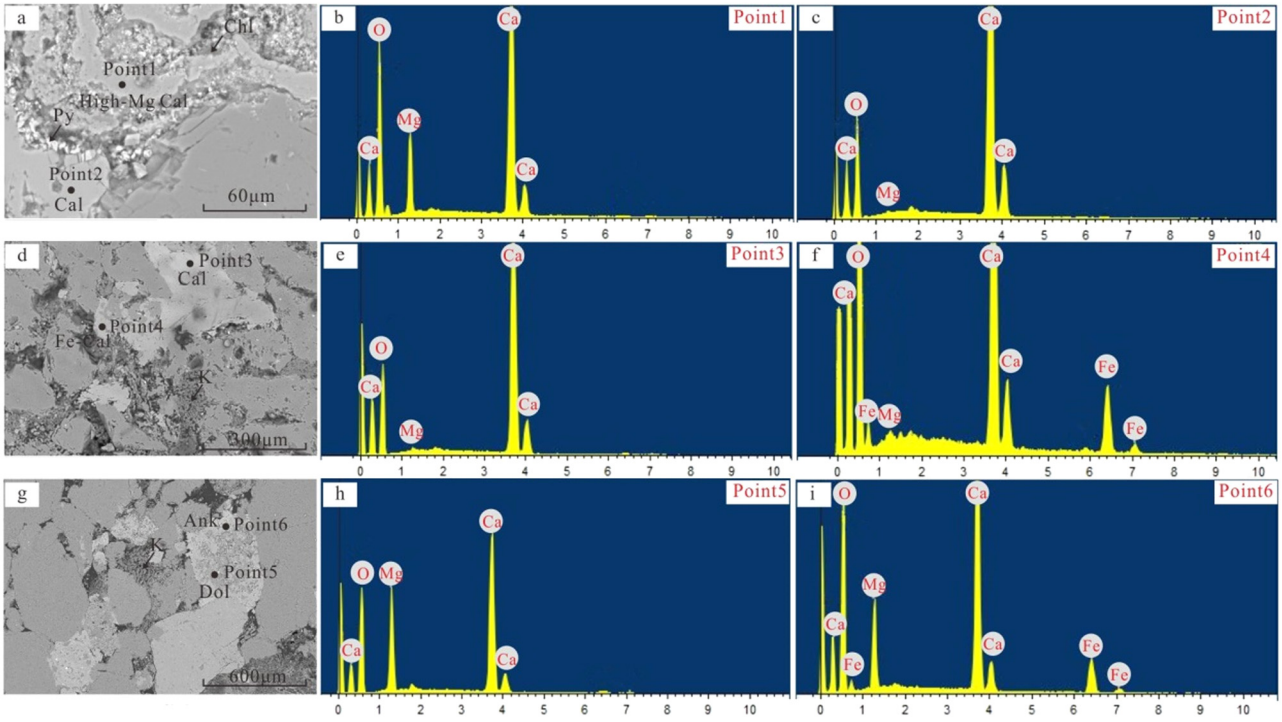

Figure 4: Electron microprobe backscatter images and energy spectrum characteristics of typical carbonate cements. (a–c) W7, 2595.5 m, characteristics of back scattering and energy spectrum of micritic high-Mg calcite and calcite in early stage; (d–f) W550, 3419.48 m, characteristics of back scattering and energy spectrum of calcite in middle stage and ferrocalcite in late stage; (g–i) W58, 3026.10 m, characteristics of back scattering and energy spectrum of dolomite in middle stage and ankerite in late stage.

4.3 Distribution characteristics of carbonate cements

In the deep sandstone of Dongying Sag, the content of early-stage micritic high-Mg calcite is low, which is only developed in a small number of samples, but its depth varies, ranging from 1,600 to 4,000 m. The early calcite is also developed in the range of 1,600–3,600 m, but mainly distributed in the depth of 1,600–2,700 m in sandstone samples buried more than 2,700 m deep. This type of carbonate is dissolved; thus, its content decreased. Calcite and dolomite in the middle stage are developed in the range of 2,000–4,500 m, and their contents decrease with the increase in burial depth. Microscopic observations showed that carbonate cement dissolution occurs in the late stage mainly in the depth range of 2,100–2,900 m, and the content of these carbonates in sandstone decreases beyond 2,900 m. In the late stage, the ferrocalcite and ankerite are mainly developed in sandstone with a depth of <3,000 m, and the development degree increases with the increase in depth (Figure 6).

Carbon and oxygen isotope analysis is a widely used method to study the material source and genetic mechanism of carbonate cements in clastic rocks [20–23]. The carbon and oxygen isotopes of different types of carbonate cements in deep sandstone reservoirs in Dongying Sag showed the following characteristics: because of the low content of early-stage micritic high-Mg calcite cements, it is difficult to obtain sufficient samples for isotopic testing. The $\delta^{13}C_{V\text{-}PDB}$‰ of the medium-coarse-grained calcite cement filling the primary pores in the early stage was 1.3–2.1‰ with an average of 1.7‰, and $\delta^{18}O_{V\text{-}PDB}$‰ was −10.5 to −7.5‰ with an average of −9.1‰ (Table 2), showing positive carbon isotope characteristics. The $\delta^{13}C_{V\text{-}PDB}$‰ of the calcite cement filling the dissolved pores of feldspar and the remaining primary pores of compaction in the middle stage was −2.2 to 3.4‰ with an average of 1.9‰, and the $\delta^{18}O_{V\text{-}PDB}$‰ was −13.5 to −9.3‰ with an average of −12.2‰; the $\delta^{13}C_{V\text{-}PDB}$‰ of the dolomite cement was −1.0 to 4.3‰ with an average of 2.8‰, and the $\delta^{18}O_{V\text{-}PDB}$‰ was −11.2 to −7.1‰ with an average value of −9.7‰ (Table 2). The carbon isotope of dolomite shows a stronger positive drift than that of calcite in the same stage. The $\delta^{13}C_{V\text{-}PDB}$‰ of ferrocalcite in the late stage was −3.3 to −2.7‰ with an average of −0.6‰, the $\delta^{18}O_{V\text{-}PDB}$‰ was −15.9 to −13.3‰ with an average of −14.8‰, the $\delta^{13}C_{V\text{-}PDB}$‰ of ankerite was −1.2 to 4.3‰ with an average of 1.6‰, and the $\delta^{18}O_{V\text{-}PDB}$‰

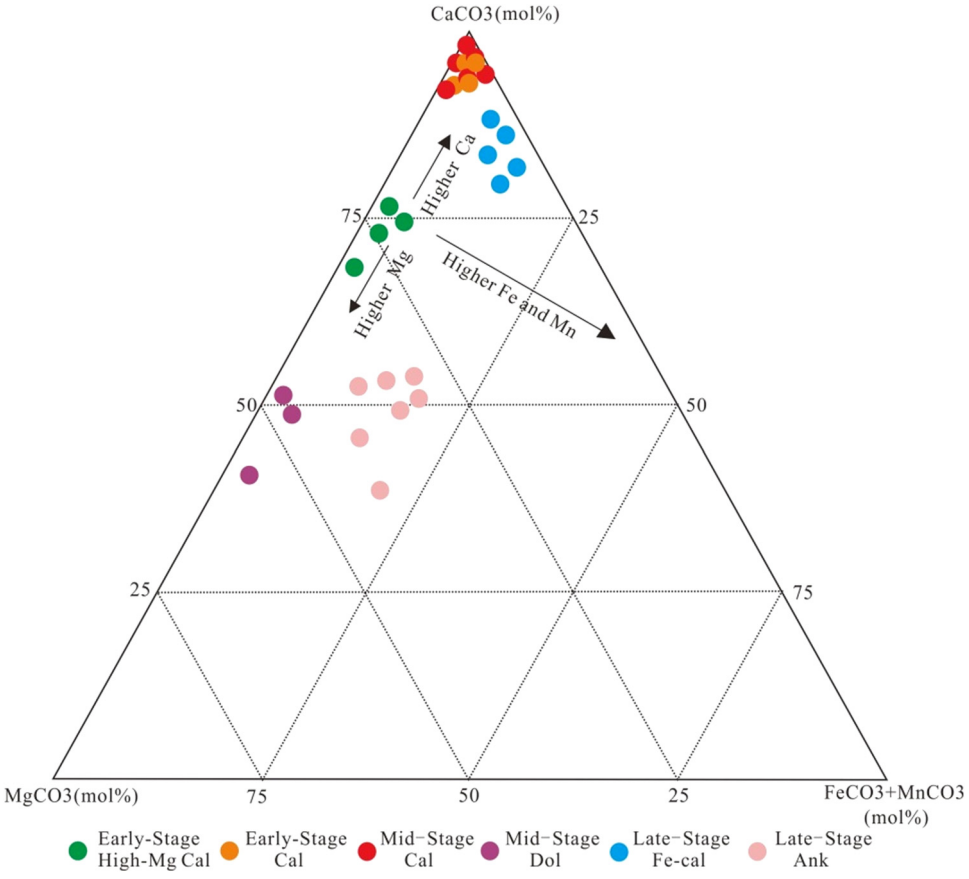

Figure 5: Composition characteristics of carbonate cements in different stages.

was –13.8 to –11.5‰ with an average of –12.7‰ (Table 2). The carbon isotope of ankerite is higher than that of ferrocalcite in the same stage.

4.4 Precipitation temperature of carbonate cement

Fluid inclusions can provide information on the precipitation temperature of authigenic minerals [10,27–29]. Due to the limited number of samples and inclusions in carbonate cements, the homogenization temperatures of fluid inclusions were detected from only a small number of middle- and late-stage carbonate cements (Figure 7a and c). The homogenization temperature of fluid inclusions in middle-stage carbonate cements mainly ranges from 95 to 120°C, while that in late-stage carbonate cements ranges from 135 to 150°C (Figure 8, Table 3). The homogenization temperature ranges of fluid inclusions in quartz grain healing fractures are mainly from 95 to 120°C and 135 to 155°C. The homogenization temperature ranges of aqueous inclusions in the enlarged edge of quartz are mainly from 100 to 115°C and 140 to 155°C (Figure 8, Table 3). According to the homogenization temperature distribution, two stages of hydrocarbon charging were identified in the deep sandstone reservoir of Dongying Sag: the precipitation temperatures of carbonate cements in the middle and late stages correspond to the two stages of hydrocarbon charging, respectively.

5 Discussion

5.1 Formation period and diagenetic sequence of carbonate cements

The $\delta^{18}O_{SMOW}$‰ of carbonate cements is controlled by the $\delta^{18}O_{SMOW}$‰ of pore fluid and formation temperature. Determining the $\delta^{18}O_{SMOW}$‰ of pore fluid is necessary to calculate the formation temperature of carbonate cements in sandstone [25,30]. During diagenesis, the pore fluid

Table 1: Composition characteristics of carbonate cements in different stages

Well	Depth (m)	Horizon	$CaCO_3$	$FeCO_3$	$MgCO_3$	$MnCO_3$	Mineral name period
W78	3426.18	Es3	97.21	1.79	0.00	0.00	Calcite middle stage
	3429.84	Es3	98.50	0.17	1.12	0.21	Calcite middle stage
N876	3372.19	Es3	90.55	8.40	1.06	0.00	Ferro-calcite late stage
	3375.20	Es3	84.59	15.41	0.00	0.00	Ferro-calcite late stage
N106	2595.21	Es3	98.21	1.79	0.00	0.00	Calcite middle stage
X154	2960.50	Es3	90.15	0.98	8.87	0.10	Calcite early stage
N105	3251.66	Es3	65.35	0.78	33.87	0.00	Calcite early stage
S127	2180.80	Es3	86.75	0.48	12.77	0.12	Calcite early stage
H144	2691.25	Es3	77.49	1.47	21.04	0.00	Calcite early stage
	2691.25	Es3	69.27	0.46	30.27	0.00	Calcite early stage
S11	3041.20	Es3	86.18	12.03	1.79	0.00	Ferro-calcite late stage
	3080.50	Es3	99.44	0.56	0.00	0.00	Calcite middle stage
H169	2840.90	Es3	51.80	0.23	47.97	0.00	Dolomite middle stage
	2945.00	Es3	31.24	0.46	68.30	0.00	Dolomite middle stage
W631	2804.00	Es3	59.42	15.07	24.18	1.34	Ankerite late stage
N24	3042.50	Es4	98.24	0.56	1.20	0.22	Calcite middle stage
	3082.11	Es4	87.49	11.47	1.04	0.00	Ferro-calcite late stage
N21	2987.20	Es3	58.47	13.35	25.87	2.31	Ankerite late stage
	3032.60	Es3	86.23	12.13	1.63	0.00	Ferro-calcite late stage
W7	2616.10	Es4	60.25	13.54	26.21	0.00	Ankerite late stage
	2616.10	Es4	50.68	15.73	32.43	1.16	Ankerite late stage
S126	2616.10	Es4	51.81	11.27	36.92	0.00	Ankerite late stage
N25	3274.10	Es3	60.90	15.46	23.13	0.51	Ankerite late stage
	3274.10	Es3	51.70	1.03	47.27	0.00	Dolomite middle stage
	3283.80	Es3	88.52	0.81	10.67	0.00	Calcite early stage
T174	2903.80	Es4	57.26	13.84	28.17	0.73	Ankerite late stage
W587	3456.40	Es4	55.34	12.04	30.69	1.93	Ankerite late stage
B656	3187.40	Es4	95.71	2.17	2.12	0.00	Calcite middle stage
Ch371	2693.85	Es4	96.11	0.79	3.10	0.00	Calcite early stage
FS6	3697.95	Es4	75.70	1.03	23.27	0.00	Calcite early stage

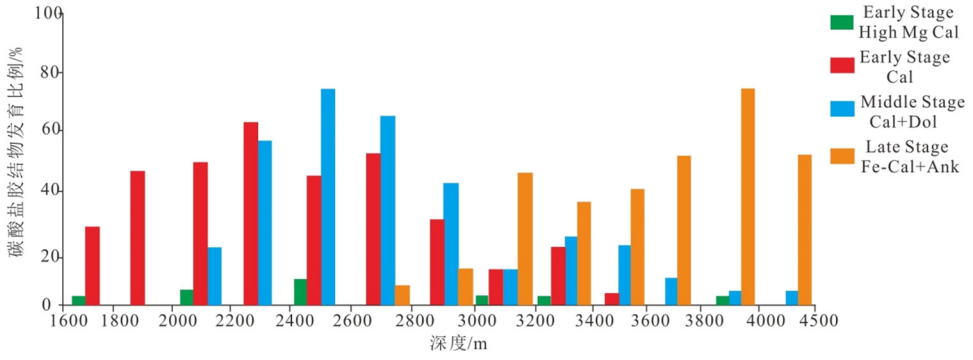

Figure 6: Vertical distribution characteristics of carbonate cements in different stages.

from the sedimentary water exchanges material with clastic particles, making the $\delta^{18}O_{SMOW}$‰ of the pore fluid significantly heavier [31,32]. The $\delta^{18}O_{SMOW}$‰ of the original sedimentary water body in Dongying Sag was −4.8‰, and the $\delta^{18}O_{SMOW}$‰ of the pore fluid became −3‰ after feldspar dissolution [32–34].

The carbonate cements in the early stage developed in the deep sandstone reservoirs in Dongying Sag are high-Mg calcite developed in mudstone and calcite filled with early intergranular primary pores. High-Mg calcite is inferred to be a paracontemporaneous diagenetic product (Figure 5) according to its composition characteristics,

Table 2: Carbon and oxygen isotope composition and oxygen isotope temperature test results of carbonate cements[(a)]

Well	Depth (m)	Strata	Type	Stage	$\delta^{13}C_{PDB}$ (‰)	$\delta^{18}O_{PDB}$ (‰)	$\delta^{18}O_{SMOW}$ (‰)	Temperature *T* (°C)
H155	2981.2	Es3	Calcite	Middle stage	3.4	−11.8	15.5	88.3
H163	2833.4	Es3	Calcite	Middle stage	2.1	−12.1	15.1	91.5
N22	3208.6	Es3	Ankerite	Late stage	−1.2	−13.0	13.9	134.9
S127	3214.5	Es3	Calcite	Middle stage	2.8	−9.3	18.7	64.2
X154	2934.5	Es3	Calcite	Early stage	1.5	−7.5	21.1	38.7
N28	3120.8	Es3	Ankerite	Late stage	2.3	−13.8	12.9	147.5
H130	2780.4	Es3	Fe-Calcite	Late stage	2.7	−13.3	13.5	106.3
	2781.6	Es3	Dolomite	Middle stage	3.7	−10.8	16.8	103.9
H156	2752.8	Es3	Dolomite	Middle stage	4.3	−11.2	16.2	109.7
L881	2969.8	Es3	Ankerite	Late stage	1.2	−12.8	14.1	132.5
W7	2597.5	Es4	Fe-Calcite	Late stage	−2.1	−15.3	10.9	134.4
	2597.5	Es4	Calcite	Late stage	2.1	−9.5	18.5	53.6
	2597.5	Es4	Calcite	Early stage	1.3	−10.5	17.2	62.0
L933	2908.7	Es3	Ankerite	Late stage	4.3	−13.0	13.9	134.9
H159	2954.3	Es3	Dolomite	Middle stage	−1.0	−10.1	17.7	95.6
N301	2780.0	Es3	Calcite	Middle stage	3.2	−13.1	13.7	104.4
	2786.5	Es3	Calcite	Middle stage	−2.2	−12.5	14.5	97.0
HX108	3478.2	Es3	Dolomite	Middle stage	3.9	−10.5	17.1	101.1
S106	3398.7	Es3	Fe-Calcite	Late stage	−3.3	−15.9	10.1	144.4
S121	3530.0	Es3	Calcite	Middle stage	1.3	−13.5	13.2	109.3
S127	3162.8	Es3	Dolomite	Middle stage	2.9	−7.1	21.6	65.3
Y67	3067.2	Es3	Calcite	Middle stage	2.5	−12.8	14.1	100.6
	3072.0	Es3	Ankerite	Late stage	1.6	−12.3	14.8	124.4
HX108	3477.0	Es3	Dolomite	Middle stage	2.8	−8.2	20.1	76.1
FS1	4322.4	Es4	Ankerite	Late stage	−0.4	−11.5	15.8	113.8
S106	3398.7	Es3	Ankerite	Late stage	3.3	−12.7	14.3	130.1
	3410.1	Es3	Fe-Calcite	Late stage	−3.1	−14.1	12.5	116.4
N21	2987.2	Es3	Fe-Calcite	Late stage	2.2	−14.7	11.6	126.2
	3032.6	Es3	Fe-Calcite	Late stage	−0.3	−15.4	10.7	136.9

[(a)] $\delta^{13}C_{PDB}$‰ is a stable carbon isotope (PDB standard); $\delta^{18}O_{PDB}$‰ is a stable oxygen isotope (PDB standard); $\delta^{18}O_{SMOW}$‰ is a stable oxygen isotope (SMOW standard). PDB is the abbreviation of Pee Dee belemnite in North America. SMOW is the standard mean seawater in Vienna. The conversion formula is $\delta^{18}O_{PDB} = 1.03086\ \delta^{18}O_{SMOW} - 30.86$ [24]. Ferrocalcite is calculated using the formula $10^3 \ln \alpha_{calcite\text{-}water} = 2.78 * 106 * T^{-2} - 2.89$ [25]; ankerite is calculated according to the formula $10^3 \ln \alpha_{calcite\text{-}water} = 2.78 * 106 * T^{-2} + 0.11$ [26].

and it was formed before the dissolution period of feldspar in the pore fluid with a $\delta^{18}O_{SMOW}$‰ of −4.8‰ (Figure 3a and b). The calcite in the early stage was also formed before feldspar dissolution in the pore fluid with a $\delta^{18}O_{SMOW}$‰ of −4.8‰ (Figure 3c and d). The $\delta^{18}O_{PDB}$‰ was −10.5 to −7.5‰. The calculated isotopic temperature (*T*°C) of carbonate cements in this stage was 38.7–62.0°C (Table 2). The carbonate cements in the middle stage are calcite and dolomite filled with feldspar dissolution pores and compacted residual pores. Because they were formed after feldspar dissolution, it was formed in the pore fluid with a $\delta^{18}O_{SMOW}$‰ of −3‰ (Figure 3e, g and h), and the $\delta^{18}O_{PDB}$‰ is −13.5 to −7.1‰. The calculated isotopic temperature (*T*°C) of carbonate cements was 64.2–109.7°C (Table 2), and the peak homogenization temperature of inclusions was 70–110°C (Figure 8). Combined with the research results of the burial history of Shahejie Formation in Dongying Sag [47], the carbonate cements in this stage are diagenetic products of the early Dongying Formation, and the temperature calculated by isotope is consistent with the measured homogenization temperature of inclusions. The carbonate cements in the late stage are ferrocalcite and ankerite, which are filled with feldspar dissolved in pores and metasomatized the secondary enlarged edges of quartz (Figure 3e, g, and h) formed in a pore fluid with a $\delta^{18}O_{SMOW}$‰ of −3‰ and $\delta^{18}O_{V\text{-}PDB}$‰ of −15.9 to −11.5‰. The calculated isotope temperature (*T*°C) of carbonate cements in this stage is 106.3–147.5°C (Table 2), and the peak homogenization temperature range of inclusions is 120–150°C (Figure 8), which coincides with each other, and they are mainly the

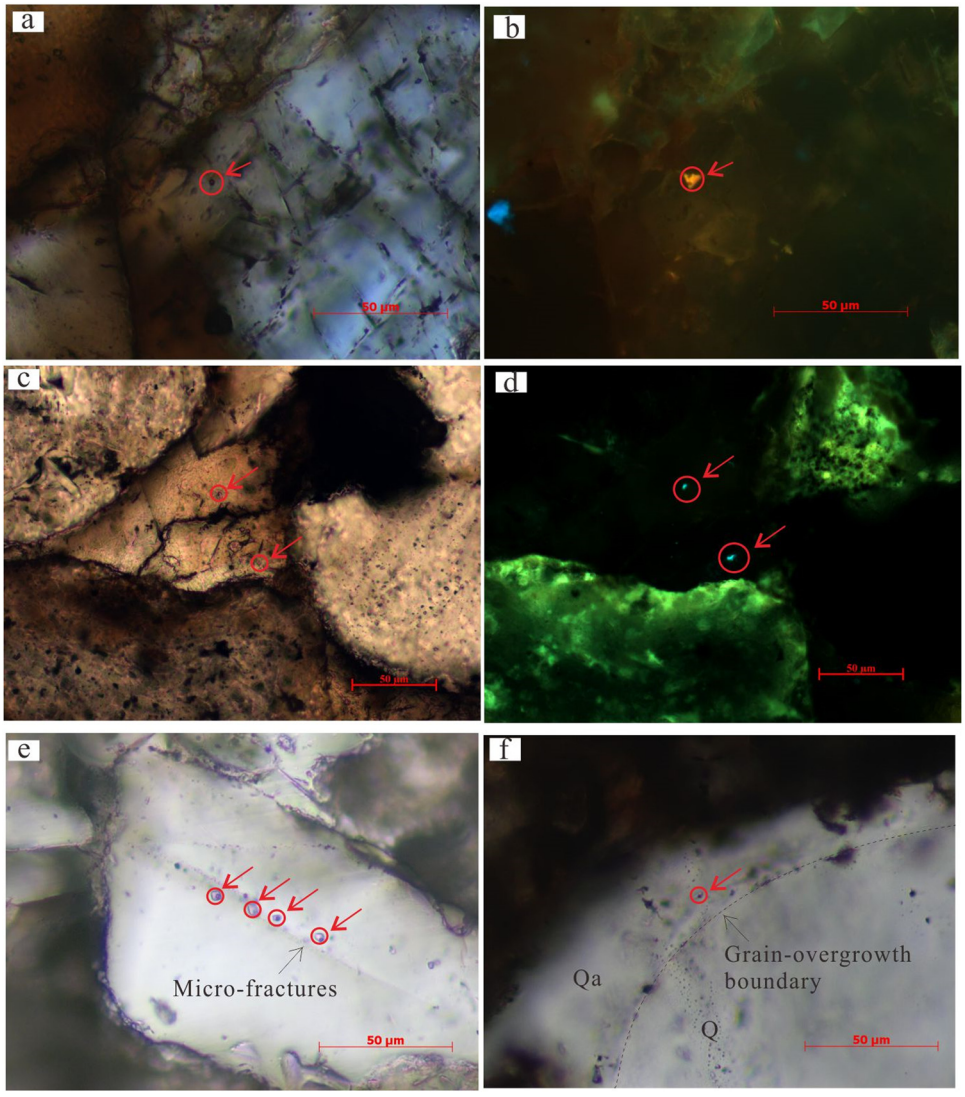

Figure 7: Inclusion characteristics of quartz and carbonate cements; (a and b) H169, 3026.50 m, hydrocarbon inclusions in carbonate cements in middle stage show yellow-white fluorescence; (c and d) N21, 2987.20 m, hydrocarbon inclusions in carbonate cements in late stage show blue-white fluorescence; (e) S136, 3214.50 m, aqueous inclusions in quartz grain healing fractures; and (f) L933, 2909.10 m, aqueous inclusions in the enlarged edge of quartz.

diagenetic products of the late Guantao Formation to the present.

Therefore, our comprehensive analyses showed that the diagenetic sequence of carbonate cements and other cements in the deep sandstone reservoir of Dongying Sag is as follows: micritic high-Mg calcite in the early stage → calcite in the early stage filled with primary pores without obvious compaction and diagenetic transformation → feldspar dissolution/quartz secondary enlargement/authigenic kaolinite precipitation → calcite and dolomite in the middle stage filled with feldspar dissolved and compacted in residual pores → ferrocalcite and ankerite in the late stage filled with the dissolution pores of calcite and dolomite in the early stage and metasomatized the enlarged edge of quartz (Figure 9).

5.2 Discussion on material source and genesis of carbonate cements

During the formation of carbonate cements, carbons in all types of organic sources are exchanged. Different types of carbon-rich acidic materials (organic acids, CO_2) are formed in different evolutionary stages of source rocks. Therefore, the carbon isotope characteristics of carbonate

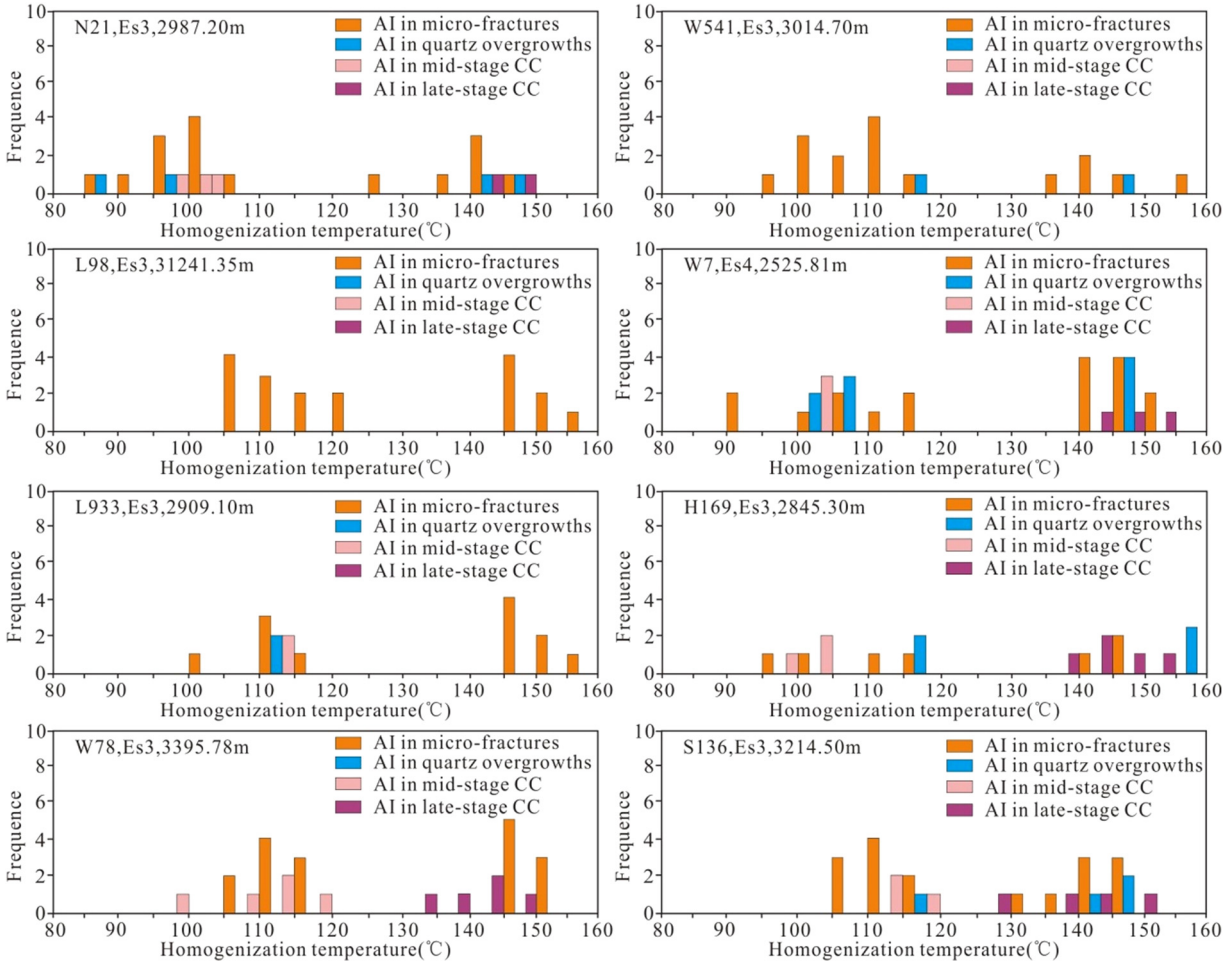

Figure 8: Characteristics of homogenization temperature distribution of inclusions in carbonate cements.

Table 3: Homogenization temperature data of aqueous inclusions in quartz and carbonate cements

Well	Depth (m)	Strata	Aqueous inclusions in microfractures in quartz Th°C (Number)	Aqueous inclusions in quartz overgrowth Th°C (Number)	Aqueous inclusions in carbonate cements Th°C (Number)
N21	2987.20	Es3	85–110(10), 129–146(6)	89–105(3), 140–145(2)	95–105(2), 140–150(2)
W541	3014.70	Es3	95–120(11), 135–159(5)	115(1), 145(1)	—
L98	3141.35	Es3	105–125(11), 145–160(7)	—	—
W7	2525.81	Es4	90–120(8), 140–155(10)	100–110(5), 145–150(4)	100–105(3), 140–155(3)
L933	2909.10	Es4	100–120(5)	110–115(2)	110(2)
H169	2845.30	Es3	98–118(4), 140–150(3)	115–120(2), 155–160(3)	95–105(3), 135–155(5)
W78	3395.93	Es3	91–115(14), 145–155(8)	—	99–119(5), 130–150(5)
S136	3214.50	Es3	105–120(9), 131–149(8)	115(1), 141–150(3)	110–120(3), 128–155(4)

Th: homogenization temperature; —: no available data.

cements can reflect the evolutionary stages of source rocks. Previous studies have shown that 60–90°C is the stage of organic acid mass formation, 90–120°C is the stage of organic acid preservation, and >120°C is the stage of organic acid destruction [35,36]. Different types of acid fluids control the geochemical properties of pore fluids and affect the formation and evolution of carbonate cements in different stages.

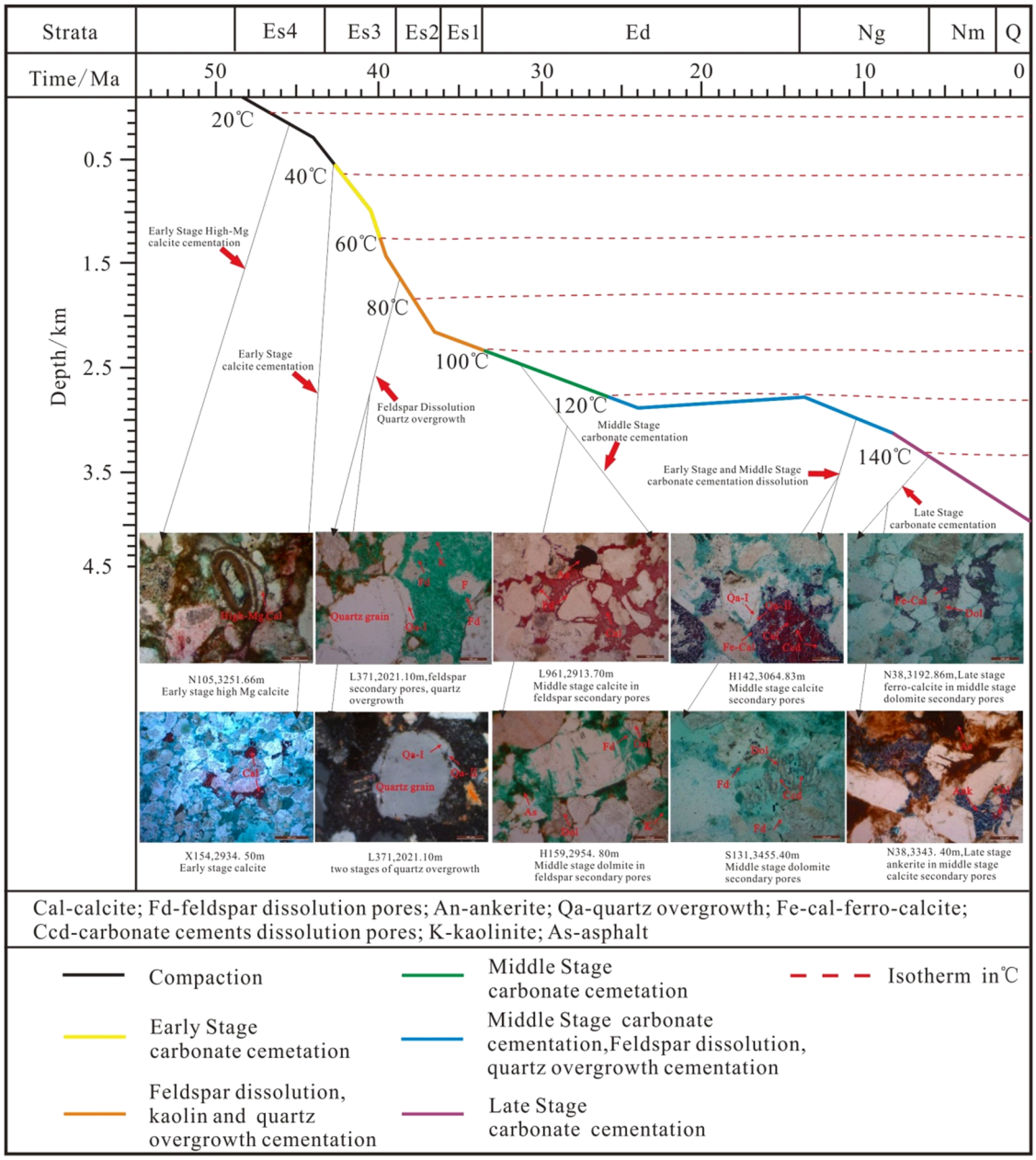

Figure 9: Sequence diagram of sandstone diagenesis in the deep Shahejie Formation of Dongying Sag (Paleogeothermal data were modified from Qiu et al., 2004; burial and thermal history were modified from Song et al., 2009).

5.2.1 Carbonate cements in the early stage

The rim-shaped argillaceous high-Mg calcite directly precipitates from the sedimentary water in the early stage and is a product of the quasi-contemporaneous period. The isotopic temperature characteristics of calcite (Figure 11a) filled with primary pores after compaction in the early stage indicate that it was formed at 38.7–62.0°C (Table 2), and the main burial depth was about 1,600–2,700 m (Figure 6). Its $\delta^{13}C_{PDB}$‰ was 1.3–2.1‰ with an average of 1.7‰, and $\delta^{18}O_{V\text{-}PDB}$‰ was −10.5 to −7.5‰ with an average of −9.1‰ (Table 2), indicating that it is a typical lacustrine carbonate (Figure 10), that is, there is no external material supply, such as microbial activity, biological organisms, or mantle-derived materials. The shale experienced obvious mechanical compaction: the main material source of carbonate cements in this stage is Ca^{2+}- and CO_3^{2-}-rich pore fluid discharged from the sedimentary source during mudstone compaction.

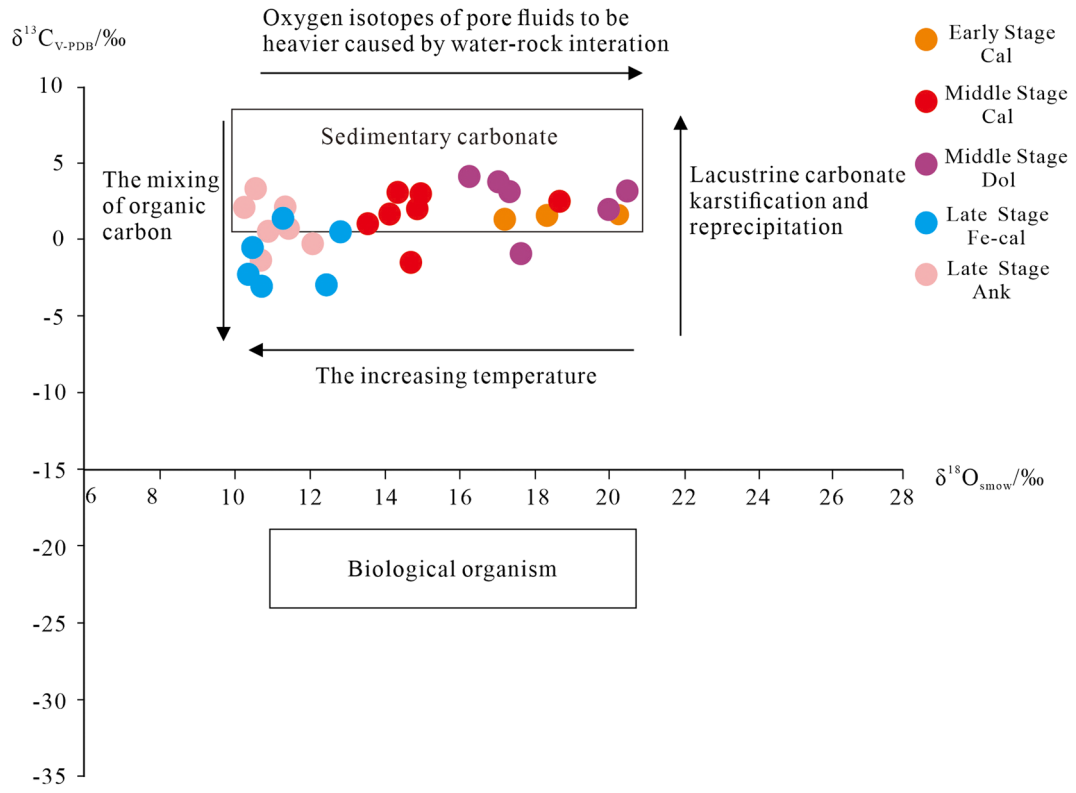

Figure 10: Isotopic characteristics of carbonate cements.

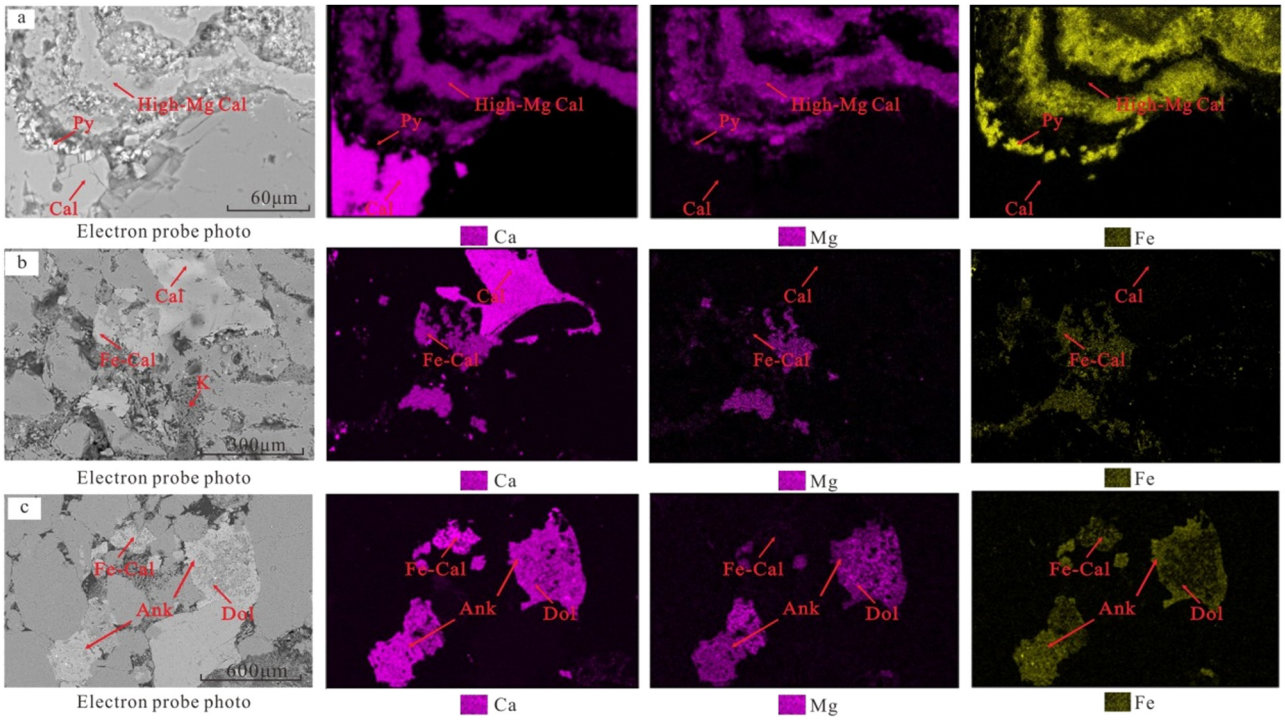

Figure 11: Electron microprobe element surface characteristics of different stages of carbonate cements. (a) W7, 2595.5 m, the micritic high-Mg calcite and calcite in early stage; (b) W550, 3419.48 m, calcite in the middle stage and ferrocalcite in the late stage filled the dissolved pores; and (c) W58, 3026.10 m, dolomite in middle stage and ankerite in the late stage filled the dissolved pores.

5.2.2 Carbonate cements in the middle stage

The carbonate cements in the middle stage are mainly calcite and dolomite filled with feldspar dissolution pores and compacted residual pores (Figure 3e, g and h), indicating that they were formed after large-scale feldspar dissolution. Isotopic and inclusion homogenization temperature characteristics indicate that middle-stage carbonate cements were formed at 70–110°C (Figure 8). The distribution range of the $\delta^{13}C_{PDB}$‰ was −2.2 to 4.3‰, and that of $\delta^{18}O_{V\text{-}PDB}$‰ was −13.5 to −7.1‰ (Table 2). The $\delta^{13}C_{PDB}$‰ of some carbonate cements in this stage is significantly higher than that of early-stage carbonate cements. The carbon isotope of dolomite is higher than that of the calcite cement in the same stage (Figure 10, Table 2).

Previous studies have shown that bacterial activity, internal carbon isotope fractionation of organic acids, and evaporation of lake water can lead to positive carbon isotope migration of carbonate cements. Since the precipitation temperature of carbonate cement measured by fluid inclusion in the study area exceeds the maximum temperature limit of microbial activity (70°C), the influence of bacterial activity is excluded. Carbon isotope fractionation within organic acids is believed to be the reason for the high $\delta^{13}C_{PDB}$‰ value [37]. The carbon and oxygen isotope measurements of lacustrine carbonate in Shahejie Formation in Dongying Sag showed that the $\delta^{13}C_{PDB}$‰ values of carbonate rocks in Es3 are mostly negative, while the $\delta^{13}C_{PDB}$‰ values of saltwater lacustrine carbonate rocks in Es4 are 1.20–6.29‰ with an average value of 3.75‰ [33,34]. We conclude that the positive carbon isotope migration of calcite in carbonate cements is due to the isotopic fractionation effect of organic acids; the positive migration of dolomite carbon isotope is mainly affected by organic acid isotope fractionation and the upwelling of high-salinity fluid in Es4. The formation process of carbonate cements in this stage is as follows: a large amount of organic matter in mudstone is formed, and organic acid is discharged. The existence of organic acid causes the dissolution of potash feldspar and plagioclase, providing a partial material source for the formation of carbonate cement in this period. Meanwhile, the overpressure fluid rich in Ca^{2+}, Mg^{+}, and part of CO_3^{2-} influenced by the organic carbon source enter the reservoir Ca^{2+} in the formation water is mixed (Figure 11b and c), leading to the precipitation of these materials in the form of medium-term carbonate cement. Due to the mixing of pore fluids from different sources, the compositions of carbonate cements are complex, including both calcite and dolomite.

5.2.3 Carbonate cements in the late stage

Carbonate cements in the late stage are mainly ferrocalcite and ankerite (Figure 3e, g and h): the distribution range of the $\delta^{13}C_{PDB}$‰ was −3.3 to 4.3‰, and that of the $\delta^{18}O_{V\text{-}PDB}$‰ was −15.9 to −11.5‰ (Table 2): the precipitation temperature range was 131.6–144.1°C (Table 3), mainly developed in sandstone with a burial depth <3,000 m (Figure 6). In the geothermal range (>120°C) of this depth, organic acids and some organic matter cracked to form a large amount of CO_2, which was transformed into CO_3^{2-} during fluid–rock interactions [35,36]. The carbonate cements in the early and middle stages had obvious dissolution (Figure 3e, g, and h) before the formation of carbonate cements in this stage, which can also provide Mg^{2+}, Ca^{2+}, and CO_3^{2-} for carbonate cements in this stage. In this diagenetic stage, the intrusion of acidic fluid rich in organic CO_2 originating from source rocks resulted in the dissolution of metamorphic rock cuttings, which could provide a large amount of Fe^{2+}. At this stage, a large amount of Ca^{2+} combined with Fe^{2+} in pore water results in the formation of ferrocalcite (Figure 11b and c). Therefore, the ferrocalcite and ankerite in the late stage are the products of CO_3^{2-} formed by organic acid splitting decomposition in late diagenesis, and Ca^{2+}, Fe^{2+}, and Mg^{2+} formed by the dissolution of metamorphic rock debris in pore fluid. Similar to the carbonate cement in the middle stage, the carbon isotope of ankerite is significantly higher than that of the corresponding ferrocalcite (Figure 10, Table 2), indicating that ferrocalcite is the product of the fluid interaction of Es3, and ankerite is affected by the high-salinity fluid from Es4.

5.3 Material exchange of carbonate cement precipitation in pore fluid

Changes in the chemical composition of the pore fluid affect composition during carbonate cement precipitation. The mudstone adjacent to the carbonate cement precipitation strata has different geochemical properties discharged during the compaction process. Formation fluids and deep hydrothermal fluids flowing up into the pores along faults can affect the properties of pore fluids,

leading to the precipitation of different types of carbonate cements. When the lake water of the Paleogene in Dongying Sag was in the quasi-contemporaneous period, the buried depth of the stratum was less than 500 m, the ground temperature was less than 40°C, the water itself involved a certain content of Ca^{2+}, Mg^{2+}, Fe^{3+}, and SO_4^{2-} [38,39], and sulfate-reducing bacteria that were widely active under geothermal conditions during this period reduced Fe^{3+} and SO_4^{2-} in water to Fe^{2+} and S^{2-} [4,40,41], combined with reduced Fe^{2+} and S^{2-}, precipitating early authigenic pyrite, which coexists with early high-Mg calcite [38,39,42]. When the continuous buried depth of the formation reaches 500–1,500 m and the ground temperature 40–60°C due to the strong compaction of the formation, Ca^{2+} and CO_3^{2-}-rich fluid in the adjacent mudstone formation is squeezed into the adjacent sandstone in the reservoir pores [43,44], leading to early-stage calcite precipitation and the filling of the primary pores of calcite particles. As the stratum is buried 1,500–2,800 m deep and the ground temperature is 60–120°C, the organic matter in the deep mudstone of Dongying Sag will generate a large amount of organic acids into the pores of sandstone, causing the dissolution of potash feldspar and plagioclase, production of K^+ and Na^+, and Ca^{2+}, Si^{4+}, and Al^{3+} ions entering the pore fluid. Among them, Si^{4+} and Al^{3+} ions migrate with the fluid and precipitate in the form of secondary enlargement of kaolinite and quartz under suitable geological conditions. At the same time, due to the fault activity at this stage, high-salinity hydrothermal fluids rich in Mg^{2+} and Ca^{2+} and the organic sources of CO_3^{2-} enter pore fluids, depositing and producing in the form of carbonate cements in the middle stage and filling the dissolved pores of potash feldspar and plagioclase.

5.4 Hydrocarbon indicating the significance of carbonate cements

The thermal evolution and diagenesis of source rocks in sedimentary basins are interactive and organic processes. Organic acids produced during the thermal evolution of the source rock directly affect the stability of carbonate cements in the overlying reservoir sandstone [36]. Therefore, the charging of hydrocarbon fluids inevitably leads to secondary changes in the reservoir, and carbonate cements and hydrocarbon inclusions present in carbonate cements can well record these changes. The content of calcite in deep sandstone reservoirs in Dongying Sag is similar in sandstone samples with and without hydrocarbon display; the content of dolomite, ferrocalcite, and ankerite in sandstone samples with hydrocarbon display is much higher than that in sandstone samples without hydrocarbon display (Figure 12). In addition, the early micritic high-Mg calcite is a product of the concentration of sedimentary water and the product of the compression fluid of the calcite mudstone filling the dissolution pores in the early stage, both of which are not symbiotic with asphaltenes and have no relation with hydrocarbon fluids. The calcite and dolomite in the middle stage are associated with asphaltenes and precipitate in the pores after feldspar dissolution (Figure 13a and b);

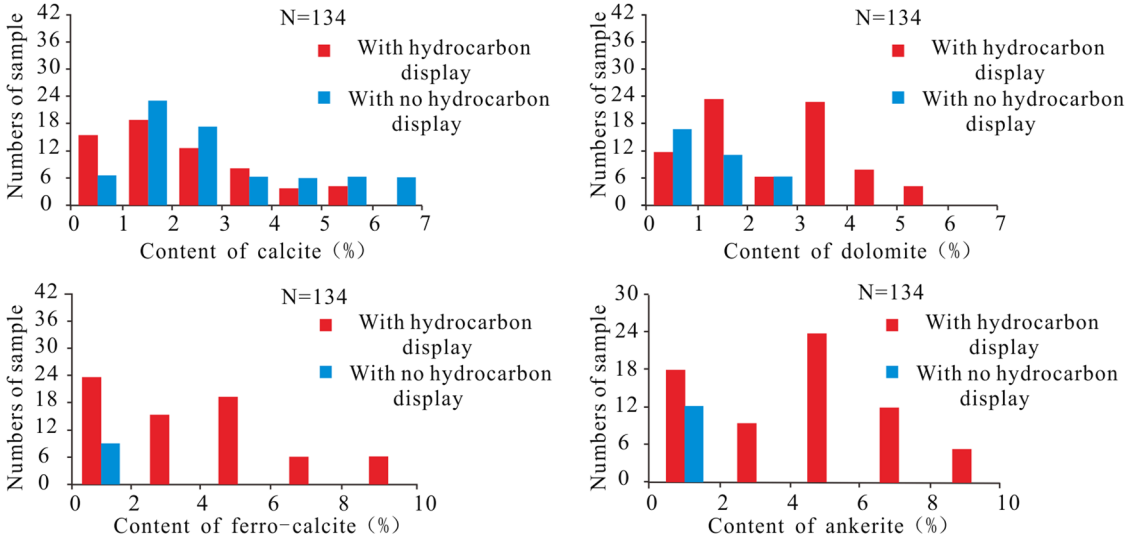

Figure 12: Relationship between the content of carbonate cements and the display of hydrocarbon.

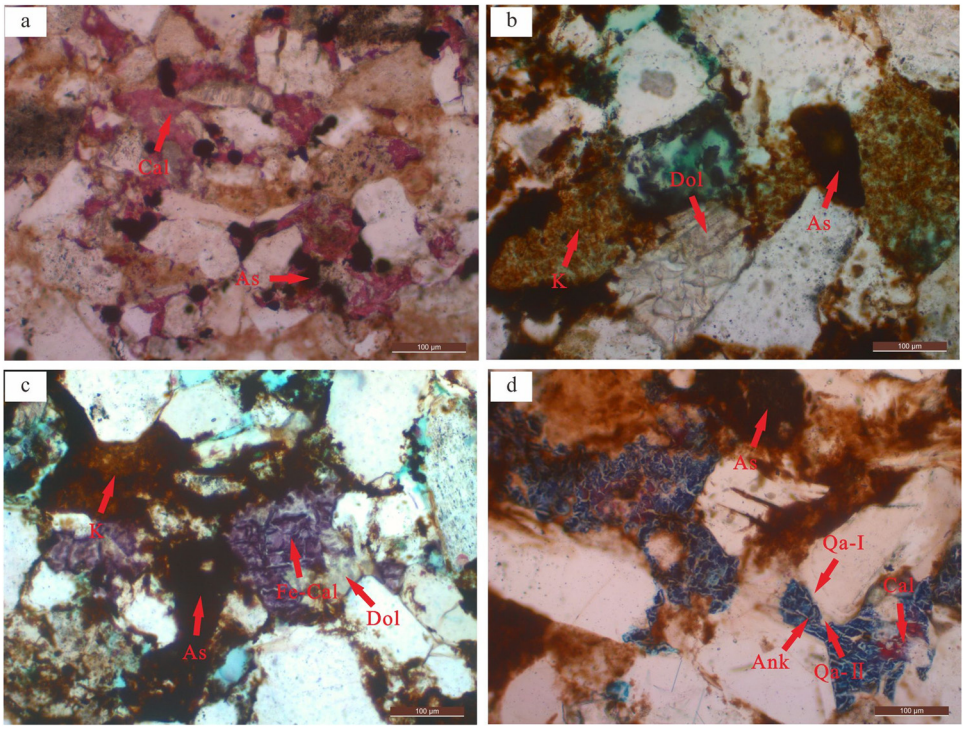

Figure 13: Relationship between carbonate cements in different stages and hydrocarbon charging; (a) H130, 2722.31 m, calcite in the middle stage associated with asphaltene; (b) W541, 3035.40 m, dolomite in the middle stage associated with asphaltene; (c) N116, 3091.64 m, ferrocalcite in the late stage associated with asphaltene; and (d) L65, 3219.20 m, ankerite in the late stage associated with asphaltene.

ferrocalcite and ankerite in the late stage are also associated with asphaltenes, filling the dissolution pores of carbonate cements in the early and middle stages (Figure 13c and d). Thus, carbonate cements in the two stages are all diagenetic products formed during the filling of hydrocarbon fluids: Dongying Sag has two periods of hydrocarbon charging, namely the early charging period of the Dongying Formation and the late Guantao Formation–the present charging period [45,46]. In this work, hydrocarbon inclusions in the early hydrocarbon charging period were recorded as yellow-brown fluorescence in middle-stage carbonate cements (Figure 7b), and the measured peak homogenization temperature range was 95–120°C (Figure 8). Combined with the research results of the burial history of Shahejie Formation in the study area [47], these results show that the carbonate cements in this stage are the early diagenetic products of Dongying Formation. It coincides with the early hydrocarbon charging period of the early Dongying Formation, proving that the carbonate cements in this stage represent the early hydrocarbon charging of Dongying Formation. During the late oil and gas charging period, the hydrocarbon inclusions were recorded in the form of blue-white fluorescence in the late carbonate cement (Figure 7d), and the measured peak homogenization temperature range was 135–150°C (Figure 8), indicating that the carbonate cements in this stage are a diagenetic product from the end of Guantao Formation to the present, indicating that the carbonate cements in this stage represent the end of Guantao Formation to the present. Hydrocarbon charging and the formation of carbonate cement precipitation in the late stage indicate continuous hydrocarbon accumulation.

6 Conclusions

(1) The deep sandstone reservoirs in Dongying Sag are mainly composed of three stages of carbonate cements. Carbonate cements in the early stage can be divided into two types: the first type is micritic high-Mg calcite, which is rim-shaped and coexists with a small amount of authigenic pyrite particles; the second type is medium-coarse-grained calcite filled with primary pores. The carbonate cements in the middle stage are calcite and dolomite filled with secondary dissolution pores of feldspar, and the carbonate cements in the late stage are ferrocalcite and ankerite filled with the dissolution pores of early and middle stage carbonate cements, respectively.

(2) The formation stages of the three stages of carbonate cements are micritic high-Mg calcite in the early stage → calcite in the early stage filled with primary pores without obvious compaction and diagenetic transformation → feldspar dissolution/quartz secondary enlargement/authigenic kaolinite precipitation → calcite and dolomite in the middle stage filled with feldspar dissolved and compacted in residual pores → ferrocalcite and ankerite in the late stage filling the dissolved pores in calcite and dolomite, and metasomatic quartz secondary enlargement.

(3) Ca^{2+}, Mg^{2+}, and CO_3^{2-} in the pore fluid in the early stage entered the rock skeleton in the form of high-Mg calcite; Ca^{2+} and CO_3^{2-} precipitate in sandstone in the form of calcite in the early stage during the compaction and drainage of mudstone; influenced by the intrusion of the overpressure of the fluid, Ca^{2+} and Mg^{2+} rich in the fluid and CO_3^{2-} that is partly affected by the organic carbon source enter the reservoir. These substances mix and precipitate with Ca^{2+} in the original formation water to form middle-stage carbonate cements. The mixing of pore fluids from different sources makes the composition of carbonate cements complex in this period, involving both calcite and dolomite; carbonate cements in the late stage are the product of the combination of CO_3^{2-} formed by organic acid splitting decomposition in late diagenesis, CO_3^{2-} formed by carbonate cement dissolution in early and middle stages, and Mg^{2+}, Ca^{2+}, and Fe^{2+} plasma formed by the dissolution of metamorphic rock cuttings in the pore fluid.

(4) High-Mg calcite and calcite in the early stage did not coexist with asphaltenes and are not related to hydrocarbon fluids. The carbonate cements in the middle and late stages are both diagenetic products formed during the charging process of hydrocarbon fluids. The carbonate cements in the middle stage are the early diagenetic products of Dongying Formation; it coincides with the early hydrocarbon charging period of the early Dongying Formation, proving that the carbonate cements in this stage represent the early hydrocarbon charging of Dongying Formation. The carbonate cements in the late stage are diagenetic products from the end of Guantao Formation to the present, which coincides with the period of hydrocarbon charging since the end of the Guantao Formation, proving that carbonate cements of this stage represent the hydrocarbon charging at the end of Guantao Formation to the current.

Acknowledgments: This study was financially supported by the National Science and Technology Special Grant (No. 2016ZX05006-003). Thanks also go to the following individuals and institutions: Dr. Yuelin Feng and Dr. Wei Meng of Shengli Oilfield Exploration and Development Research Institute of Sinopec; Shengli Oilfield Company of Sinopec provided all the related core samples and some geological data of Dongying Sag.

Funding information: This study was financially supported by the National Science and Technology Special Grant (No. 2016ZX05006-003).

Author contributions: Yuelin Feng and Wei Meng designed the experiments; Hongwei Han, Jingqiang Yu, and Weizhong Zhang carried them out. Shuli Li and Xiaochen Li drew the figures and carried out the tables. Ping Gao reviewed and edited. Tianjiao Zhang offered the article thoughts and prepared the full manuscript with contributions from all co-authors. The authors applied the SDC approach for the sequence of authors.

Conflict of interest: Authors state no conflict of interest.

References

[1] Carlos R, Rafaela M, Karl R, Permanyer A. Facies-related diagenesis and multiphase siderite cementation and dissolution in the reservoir sandstones of the Khatatba Formation Egypt western desert. J Sediment Res. 2001;71:459–72.

[2] Beavington-Penney SJ, Nadin P, Wright VP, Clarke E, McQuilken J, Bailey HW. Reservoir quality variation on an Eocene carbonate ramp El Garia formation offshore Tunisia: Structural control of burial corrosion and dolomitisation. Sediment Geol. 2008;209:42–57.

[3] Brigraud B, Durlet C, Deconinck J, Vincent B, Thierry J, Trouiller A. The origin and timing of multiphase cementation in carbonates: impact of regional scale geodynamic events on the middle Jurassic limestones diagenesis (Paris Basin France). Sediment Geol. 2009;222:161–80.

[4] Liu D, Sun X, Li Z, Tang N, Tan Y. Carbon and oxygen isotope analysis of fluid inclusions in Ordovician carbonate veins of Ordos Basin. Acta Pet Sin. 2007;28:68–72.

[5] Sun ZX, Sun ZL, Lu HJ, Yin XJ. Characteristics of carbonate cements in sandstone reservoirs: a case from Yanchang formation middle and southern Ordos Basin China. Pet Explor Dev. 2010;37:543–51.

[6] Yang Z, Zou CN, He S, Li QY, He ZL, Wu HZ, et al. Formation mechanism of carbonate cemented zones adjacent to the top overpressured surface in the central Junggar Basin NW China. Sci. China: Earth Sci. 2010;53:529–40.

[7] You L, Li C, Zhang Y. Distribution and genetic mechanism of carbonate cements in the Zhuhai formation reservoirs in Wenchang-A sag pear river mouth basin. Oil Gas Geol. 2012;33:883–2.
[8] Guo J, Zeng J, Song G, Zhang Y, Meng W. Characteristics and origin of carbonate cements of Shahejie formation of central uplift belt in Dongying depression. China Earth Sci. 2014;39:565–76.
[9] Liu SB, Huang SJ, Shen ZM, Lu ZX, Song RC. Diagenetic fluid evolution and water-rock interaction model of carbonate cements in sandstone: an example from the reservoir sandstone of the fourth member of the Xujiahe formation of the Xiaoquan-Fenggu area Sichuan Province. Sci China: Earth Sci. 2014;57:1077–92.
[10] Han YJ, He S, Song GQ, Luo SY. Origin of carbonate cements in the overpressured top seal and adjacent sandstones in Dongying depression. Acta Pet Sin. 2012;33:385–93.
[11] Hao F, Sun YC, Li ST, Zhang QM. Overpressure retardation of organic-matter maturation and petroleum generation: a case study from the Yinggehai and Qiongdongnan Basins South China Sea. AAPG Bull. 1995;9:551–62.
[12] Wang Q, Hao LW, Chen GJ, Zhang GC, Zhang R, Ma XF, et al. Forming mechanism of carbonate cements in siliciclastic sandstone of Zhuhai Formation in Baiyun Sag. Acta Pet Sin. 2010;1:553–2.
[13] Bourdet J, Pironon J, Levresse G. Petroleum accumulation and leakage in a deeply burried carbonate reservoir nispero field (Mexico). Mar Pet Geol. 2010;27:126–42.
[14] Baron M, Parnell J, Mark D, Carr A, Przyjalgowski M, Feely M. Evolution of hydrocarbon migration style in a fractured reservoir deduced from fluid inclusion data clair field west of Shetland UK. Mar Pet Geol. 2008;25:153–72.
[15] Roedder E. Fluid inclusion. In: MSO America, editors. Reviews in Mineralogy. Washington: Mineralogical Society of America; 1984.
[16] Liu Q, Zhang LY, Shen ZM, Kong XX, Li Z. Evolution of lake-basin types and occurrence of hydrocarbon source rocks in Dongying depression. Acta Pet Sin. 2004;25:42–5.
[17] Li L, Zhong DL, Shi XP. Cenozoic uplifting/subsidence coupling between the West Shandong Rise and the Jiyang Depression Northern China. Acta Geol Sin (Chin Ed). 2007;81:1215–28.
[18] Yang HZ, Ren JY. Tectonic styles and kinematic characteristics of negative inversion structure in Dongying depression. China Earth Sci. 2009;29:2808–15.
[19] Lu SQ, Chen GJ, Wu KY, Feng DY. Tectonic feature and evolution mechanism of central anticline belt of Dongying Sag Bohai Bay Basin. Pet Geol Exp. 2013;35:274–9.
[20] Sun ZX, Sun ZL, Lu HJ. Characteristics of carbonate cements in sandstone reservoirs: a case from Yanchang Formationmiddle and southern Ordos Basin China. Pet Explor Dev. 2010;37:543–51.
[21] Tian YM, Shi ZJ, Song JH, Wu XM, Hong CY. Characteristics of carbonate cements of Member 8 of Yanchang Formation in the Yichuan-Xunyi area Ordos Basin China. J Chengdu Univ Technol. 2011;38:378–84.
[22] Tan XF, Huang JH, Li J, Gao HC, Kuang H, Jiang W. Origin of carbonate cements and the transformation of the reservoir in sandstone under the deep burial condition: a case study on Eocene Kongdian formation in Jiyang depression Bohai Bay Basin. Geol Rev (Beijing, China). 2015;61:1107–20.
[23] Shen ZH, Yu BS, Han SY, Yang ZH, Huang ZH. Application of thermodynamic equilibrium of dissolution and precipitation of carbonate cement in prediction of clastic reservoir quality – a case study of Es3 in Bonan sag. J Northeast Pet Univ. 2018;5:63–72.
[24] Qiang ZT. Carbonate Reservoirs Geology. Beijing, China: Petroleum University Publication; 1998.
[25] Friedman I, O'Neil JR. Compilation of stable isotopic fractionation factors of geochemical interest. In: Fleischer M, editor. Data of Geochemistry. U.S. Geological Survey Professional Paper 440KK 12; 1977.
[26] Fisher SR, Land LS. Diagenetic history of the Ecocene Wilcox sandstones and associated formation waters south central texas. Geochim Cosmochim Acta. 1986;60(Suppl.):551–62.
[27] Parnell J, Carey PF, Monson B. Fluid inclusion constraints on temperatures of petroleum migration from authigenic quartz in Bitumen Veins. Chem Geol. 1996;129:217–26.
[28] Yu ZC, Liu KY, Zhao MJ, Liu SB, Zhuo QG, Lu XS. Characterization of diagenesis and the petroleum charge in Kela 2 Gas field Kuqa depression Tarim Basin. J China Univ Geosci. 2016;3:533–45.
[29] Lu H, Xu CG, Wang QB, Du XF, Liu XJ. Genetic mechanism of carbonate cements and its impact on the Mesozoic clastic reservoir quality of the C12 and Q17 structures, Bohai Sea Area. Oil Gas Geol. 2019;40:1270–80.
[30] Matthews A, Katz A. Oxygen isotope fractionation during the dolomitization of calcium carbonate. Geochim Cosmochim Acta. 1977;41:1431–8.
[31] Fayek M, Harrison TM, Grove M, Mckeegan KD, Coath CD, Boles JR. In situ stable isotopic evidence for protracted and complex carbonate cementation in a petroleum reservoir North Coles Levee San Joaquin Basin California USA. J Sediment Res. 2001;71:444–58.
[32] Li XY, Yuan GH, Gluyas J, Xi KL, Cao YC, Norman O, et al. Diagenesis and reservoir quality evolution of the Eocene sandstones in the northern Dongying Sag Bohai Bay Basin East China. Mar Pet Geol. 2015;62:77–89.
[33] Cai GQ, Guo F, Liu XT, Sui SL. Carbon and oxygen isotope characteristics and palaeoenvironmental implications of Lacustrine carbonate rocks from the Shahejie formation in the Dongying Sag. Ti Ch'iu Yu Huan Ching. 2009;37:347–54.
[34] Liu CL. Carbon and oxygen isotopic compositions of lacustrine carbonates of the Shahejie formation in the Dongying depression and their Paleolimnological significance. Acta Sedimentol Sin. 1998;16:109–14.
[35] Surdam RC, Boese SW, Crossey GJ. The chemistry of secondary porosity. AAPG Bull. 1984;37:127–51.
[36] Surdam RC, Crossey LJ, Hagen ES. Organic-inorganic and sandstone diagenesis. AAPG Bull. 1989;73:1–23.
[37] Franks SG, Diss RF, Freeman KH, Boles JR, Jordan ED. Carbon isotopic composition of organic acids in oil field waters San Joaquin Basin California USA. Geochim Cosmochim Acta. 2001;65:1301–10.
[38] Lu XC, Hu WX, Fu Q, Zhang WL, Zhou GJ, Hong ZH, et al. Study of salinity evolution of geofluids during syngenesis and diagenesis using composition of carbonate minerals. Acta Sedimentol Sin. 1998;16:120–6.
[39] Chen ZH, Zha M, Jin Q. Mineral elemental response to the evolution of terrestrial Brine faulted-basin: a case study in the Paleogene of well Haoke-1 Dongying Sag. Acta Sedimentol Sin. 2008;26:925–32.
[40] Boetius A, Suess E. Hydrate ridge: a natural laboratory for the study of microbial life fueled by methane from near surface gas hydrates. Chem Geol. 2004;205:291–310.

[41] Teichert BMA, Torres ME, Bohrmann G, Eisenhauer A. Fluid sources fluid pathways and diagenetic reactions across an accretionary prism revealed by Sr and B geochemistry. Earth Planet Sci Let. 2005;239:106–21.
[42] Popp BN, Wilkinson BH. Holocene lacustrine ooids from Pyramid lake Nevada. In: Peryt T, editor. Coated grains. Heidelberg: Springer-Verlag; 1983. p. 141–53.
[43] Zhao J. Laws of mudstone compaction on the west slope of the Songliao Basin. Oil Gas Geol. 2010;31:486–92.
[44] Goulty NR, Sargent C, Andras P, Aplin AC. Compaction of diagenetically altered mudstones – Part 1: Mechanical and chemical contributions. Mar Pet Geol. 2016;77:703–13.
[45] Zhu GY, Jin Q, Dai JX, Zhang SC, Guo CC, Zhang LY, et al. A study on periods of hydrocarbon accumulation an distribution pattern of oil and gas pools in Dongying depression. Oil Gas Geol. 2004;25:209–15.
[46] Li ZQ, Chen HH, Liu HM, Hao GL, Cai LM. Division of hydrocarbon charges and charging date determination of Sha 3 member Dongying depression by various aspects of fluid inclusions. Geol Sci Technol Inf. 2008;27:69–74.
[47] Song GQ, Jiang YL, Liu H, Cai DM. Pooling history of cracked gas inmiddle-deep reservoirs in Lijin-Minfeng area of the Dongying Sag. Nat Gas Ind (Chengdu, China). 2009;29:14–7.